**Title**

Effects of discreteness of chorus waves on quasilinear diffusion-based modeling of energetic electron dynamics



**Journal**

Journal of Geophysical Research Space Physics, 119(11)

**ISSN**

2169-9380

**Authors**

Tao, Xin
Bortnik, Jacob
Albert, Jay M
et al.

**Publication Date**

2014-11-01

**DOI**

10.1002/2014ja020022

Peer reviewed

AGU PUBLICATIONS

JGR

Journal of Geophysical Research: Space Physics

RESEARCH ARTICLE
10.1002/2014JA020022

**Key Points:**

- Discreteness of chorus can make quasilinear theory not applicable
- Nonlinear effects are important when chorus amplitude is large
- Quasilinear model is applicable when element amplitude and separation are small

**Correspondence to:**
X. Tao,
xtao@ustc.edu.cn

**Citation:**
Tao, X., J. Bortnik, J. M. Albert, R. M. Thorne, and W. Li (2014), Effects of discreteness of chorus waves on quasilinear diffusion-based modeling of energetic electron dynamics, *J. Geophys. Res. Space Physics*, *119*, 8848–8857, doi:10.1002/2014JA020022.

Received 27 MAR 2014
Accepted 17 OCT 2014
Accepted article online 22 OCT 2014
Published online 6 NOV 2014

# Effects of discreteness of chorus waves on quasilinear diffusion-based modeling of energetic electron dynamics

**Xin Tao[1,2,3], Jacob Bortnik[1], Jay M. Albert[4], Richard M. Thorne[1], and Wen Li[1]**

[1]Department of Atmospheric and Oceanic Sciences, University of California, Los Angeles, California, USA, [2]CAS Key Laboratory of Geospace Environment, Department of Geophysics and Planetary Sciences, University of Science and Technology of China, Hefei, China, [3]Mengcheng National Geophysical Observatory, School of Earth and Space Sciences, University of Science and Technology of China, Hefei, China, [4]Air Force Research Laboratory, Space Vehicles Directorate, Kirtland Air Force Base, Albuquerque, New Mexico, USA

**Abstract** Chorus waves are typically observed as a series of discrete, narrowband rising or falling tone elements, as opposed to a continuous uniform band, as it is often modeled. The effects of this discreteness on the applicability of quasilinear theory to interactions between electrons and parallel-propagating chorus waves in a dipole field are investigated using test particle simulations. Previous work indicated that quasilinear theory might not be directly applicable, because chorus elements are coherent or quasi-coherent. Nonlinear processes such as phase trapping and bunching were demonstrated by modeling a chorus element using a single wave. Here we represent a chorus wave field with a series of coherent elements with subpacket structures using a previously developed method involving test particle simulations to explore the applicability of quasilinear theory. By comparing electron distribution functions from test particle simulations and quasilinear predictions, we demonstrate that, besides the wave amplitude, the discreteness of chorus waves also affects the applicability of quasilinear theory. When chorus elements are close to each other and the wave amplitude is small, quasilinear theory can well describe the evolution of the electron distribution. However, when chorus elements are widely separated in space and time, the discreteness of chorus might reduce the possibility of resonant interactions between electrons and chorus. Nonlinear effects of chorus waves on electrons are also shown using the current model. The method presented in this work should be helpful for investigating the applicability of quasilinear theory in general situations. Our results should be important to understanding and modeling electrons dynamics due to interactions with chorus.

## 1. Introduction

Chorus waves are whistler mode emissions frequently observed in planetary magnetospheres [*Burtis and Helliwell*, 1976; *Hospodarsky et al.*, 2008]. Observations have shown that chorus consists of a series of elements rising or falling in frequency [*Burtis and Helliwell*, 1976; *Santolík et al.*, 2003; *Tsurutani et al.*, 2009]. The spectrogram of chorus frequently exhibits a power minimum around half of the equatorial electron cyclotron frequency, dividing chorus waves into an upper band and a lower band [*Tsurutani and Smith*, 1974].

There is now considerable interest in understanding how chorus waves affect energetic electron dynamics in the inner magnetosphere. Previous research has shown that chorus can stochastically accelerate energetic electrons into the MeV energy range, enhancing relativistic electron fluxes by an order of magnitude within about 1 day in the outer radiation belt [*Horne et al.*, 2005a, 2005b; *Reeves et al.*, 2013; *Thorne et al.*, 2013; *Hajra et al.*, 2014]. Loss of relativistic electrons in the form of MeV electron microburst has also been associated with interactions between electrons and chorus [*Thorne et al.*, 2005; *Kersten et al.*, 2011; *Lorentzen et al.*, 2001; *O'Brien et al.*, 2004; *Saito et al.*, 2012]. Storm time convection [*Gonzalez et al.*, 1994] can transport plasma sheet electrons into the inner magnetosphere. Pitch angle scattering of these energetic electrons by chorus can form frequently observed electron pancake distributions [*Su et al.*, 2009; *Tao et al.*, 2011a] and generate the diffuse aurora [*Thorne et al.*, 2010] and the pulsating aurora [*Nishimura et al.*, 2010].

Quasilinear theory has been the major tool to model the effects of chorus on energetic electrons by ignoring the fine structures in the waves. The average wave power spectrum obtained from observation is used to calculate quasilinear diffusion coefficients, which are required to solve the quasilinear diffusion equation to model the evolution of electron phase-space density [*Horne et al.*, 2005a; *Li et al.*, 2007; *Tao et al.*, 2008; *Albert et al.*, 2009; *Xiao et al.*, 2010; *Subbotin et al.*, 2010]. For example, *Horne et al.* [2005a] used quasilinear theory to estimate the acceleration time-scale of MeV electrons in the outer radiation belt due to interactions with chorus and found consistency with observations. *Albert et al.* [2009] have performed three dimensional modeling of radiation belt electron dynamics using quasilinear theory and found that chorus can produce enhanced phase space density frequently observed in the recovery phase of storms.

One of the basic assumptions of quasilinear theory is that the wave field is broadband and incoherent, so that particles move stochastically in phase space [*Kennel and Engelmann*, 1966]. However, chorus waves consist of discrete coherent or quasi-coherent elements [*Santolík et al.*, 2003, 2004; *Tsurutani et al.*, 2009, 2011], which is inconsistent with the assumption of quasilinear theory. Several studies [e.g., *Inan et al.*, 1978; *Bell*, 1984; *Omura et al.*, 2007; *Albert*, 2000; *Bortnik et al.*, 2008; *Tsurutani et al.*, 2011; *Bellan*, 2013] have demonstrated that nonlinear effects might be very important when describing interactions between electrons and a coherent wave in a dipole-like magnetic field. *Tsurutani et al.* [2013] also suggested that coherent interactions between electrons and chorus waves are important for the formation of electron microburst. Most of the theoretical and numerical investigations when applied to chorus, however, are limited to interactions between electrons and one chorus element. Hence, the overall effects of a chorus wave field, which consists of a series of discrete elements, are yet to be determined.

In the remainder of the paper, we analyze a chorus wave field consisting of a series of discrete elements using a test particle simulation, and investigate the applicability of quasilinear theory to modeling the effects of chorus on energetic electrons. In Section 2, we introduce our simulation setup and describe the method of modeling chorus waves. We then briefly review the method of solving the quasilinear diffusion equation, using the time-forward stochastic differential equation (SDE) method, in Section 3. Comparisons between quasilinear theory and test particle simulations for three different cases are shown in Section 4. Finally, we summarize our work and discuss its implications in Section 5.

## 2. Simulation Model

Test particle simulations are used to investigate the effects of chorus on electrons moving in a dipole magnetic field. Since we are only interested in the gyromotion and bounce motion of electrons, the essential feature of Earth's dipole field that we retain is the variation of magnetic field strength along a field line [*Bell*, 1984; *Tao et al.*, 2011b, 2012a]. We use a Cartesian coordinate system in the simulation, where the $z$ coordinate is equivalent to the distance along the field line from the equatorial plane in a dipole field. Latitude ($\lambda$) is also used to facilitate the interpretation of our simulation results, and it is related to the $z$ coordinate by

$$\mathrm{d}z = LR_{\mathrm{E}}(1 + 3\sin^2\lambda)^{1/2}\cos\lambda\,\mathrm{d}\lambda, \tag{1}$$

where $L$ is the $L$ shell value and $R_E$ is the Earth radius. The $z$ component of the background magnetic field $\boldsymbol{B}_0$ is a function of $\lambda$ or $z$ only,

$$B_{0z}(\lambda) = B_{0z}(\lambda = 0)\sqrt{1 + 3\sin^2\lambda}/\cos^6\lambda. \tag{2}$$

We choose $B_{0x} = -x(\mathrm{d}B_{0z}/\mathrm{d}z)/2$ and $B_{0y} = -y(\mathrm{d}B_{0z}/\mathrm{d}z)/2$ so that $\nabla \cdot \boldsymbol{B}_0 = 0$. The cold electron density is given by $n_e = n_{e0}\cos^{-4}\lambda$, following *Denton et al.* [2002]. In our simulations below, we choose $L = 5$, about the center of the outer radiation belt, and $n_{e0} = 15\,\mathrm{cm}^{-3}$.

The chorus wave fields used in our simulations consist of a series of parallel-propagating coherent rising tone elements with realistic subpacket structures as shown in Figure 1, where each element is modeled using the method described by *Tao et al.* [2012a]. The wave field is created by continuously launching a series of elements from the equatorial plane into both hemispheres until the end of simulation. These elements are identical except for the initial wave phase, which is chosen randomly. This method of creating chorus waves is consistent with previous observations that chorus waves are generated near the minimum B region along a field line [*Santolík et al.*, 2004; *Roederer*, 1970; *Tsurutani and Smith*, 1977; *Lauben et al.*, 1998; *LeDocq et al.*, 1998; *Burtis and Helliwell*, 1976; *Tsurutani et al.*, 2009]. The time difference between the launch of two successive elements is $\delta t$, as illustrated in Figure 1. The actual number of the generated chorus elements depends on the total simulation time and $\delta t$. The amplitude information and hence the subpacket structures of each chorus element are obtained from Time History of Events and Macroscale

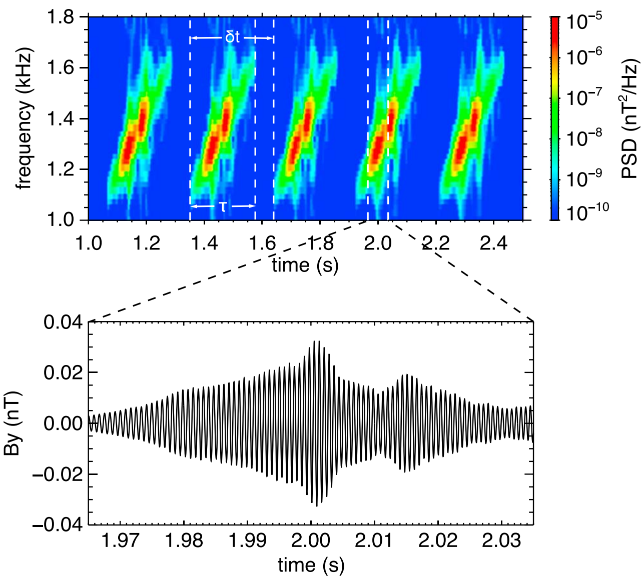


**Figure 1.** (top) The spectrogram of the modeled chorus wave field used in test particle simulations, produced using wave fields observed at $\lambda = 13.5°$. The amplitude information of chorus is obtained from an arbitrarily chosen chorus element observed by THEMIS D on 16 November 2008, and the simulation starts at $t = 0$. (bottom) The $B_y$ component of one chorus element showing subpacket structure.

Interactions during Substorms (THEMIS) [*Angelopoulos*, 2008] data using methods described in *Tao et al.* [2012a]. After generation, the amplitude of each element is assumed to be independent of latitude. The wave field is assumed to be located between −15° and 15° in latitude, following the nightside chorus wave model of *Horne et al.* [2005a]. We launch particles in the simulation after the first element generated on the equatorial plane reaches $\lambda = 15°$.

Test particles in each run below are initialized with an arbitrarily chosen equatorial pitch angle $\alpha_0 = 45°$ and energy $E = 100$ keV. All particles are placed uniformly between their two mirroring points with a random initial direction of parallel velocity and a random gyrophase. In each case, we trace the trajectories of 2000 electrons by solving the relativistic Lorentz equations using the Boris method [*Birdsall and Langdon*, 2004, pp. 356–357] for one unperturbed bounce period, which is about 0.7 s, with a time step of 1/50 of the equatorial gyroperiod. The resulting pitch angle distributions of the test particles are compared with that from quasilinear theory. For simplicity, we ignored the comparison of distributions in energy or momentum, since these variations are related to the changes in pitch angle via the single-wave characteristic surface [e.g., *Walker*, 1993, Chapter 8]. This approach can help identify the source of discrepancy, if any, between simulations and the theory. The quasilinear prediction of electron distributions is calculated using the time forward stochastic differential equations (SDE) method [*Tao et al.*, 2008] as briefly described below.

## 3. The Time Forward SDE Method

In the framework of quasilinear theory, the evolution of the bounce-averaged electron distribution $f$ as a function of equatorial pitch angle $\alpha_0$ and momentum $p$ can be obtained from the following bounce-averaged quasilinear diffusion equation

$$\frac{\partial f}{\partial t} = \frac{1}{Gp}\frac{\partial}{\partial \alpha_0} G\left(D_{\alpha_0\alpha_0}\frac{1}{p}\frac{\partial f}{\partial \alpha_0} + D_{\alpha_0 p}\frac{\partial f}{\partial p}\right) + \frac{1}{G}\frac{\partial}{\partial p} G\left(D_{\alpha_0 p}\frac{1}{p}\frac{\partial f}{\partial \alpha_0} + D_{pp}\frac{\partial f}{\partial p}\right), \tag{3}$$

where $D_{\alpha_0\alpha_0}$, $D_{\alpha_0 p}$, and $D_{pp}$ are the bounce-averaged pitch angle, mixed and momentum diffusion coefficients, respectively. Here $G$ is a Jacobian factor, $G = p^2 T(\alpha_0)\sin(\alpha_0)\cos(\alpha_0)$, and $T(\alpha_0) \approx 1.30 - 0.56\sin(\alpha_0)$ is the normalized bounce period. To use the time forward SDE method, we first set $F = Gf$ and write the diffusion equation as

$$\frac{\partial F}{\partial t} = \frac{\partial^2}{\partial \alpha_0^2}\left(\frac{D_{\alpha_0\alpha_0}}{p^2}F\right) + 2\frac{\partial^2}{\partial \alpha_0 \partial p}\left(\frac{D_{\alpha_0 p}}{p}F\right) + \frac{\partial^2}{\partial p^2}\left(D_{pp}F\right) - \frac{\partial}{\partial \alpha_0}\left(b_{\alpha_0}F\right) - \frac{\partial}{\partial p}\left(b_p F\right). \tag{4}$$

The diffusion equation in this form can be converted to time forward SDEs describing stochastic changes of the particles $\alpha_0$ and $p$, as given by *Tao et al.* [2008],

$$\mathrm{d}A_0(t) = b_{\alpha_0}(t, A_0, P)\,\mathrm{d}t + \sigma_{11}\,\mathrm{d}W_1 + \sigma_{12}\,\mathrm{d}W_2, \tag{5}$$

$$\mathrm{d}P(t) = b_p(t, A_0, P)\,\mathrm{d}t + \sigma_{21}\,\mathrm{d}W_1 + \sigma_{22}\,\mathrm{d}W_2. \tag{6}$$

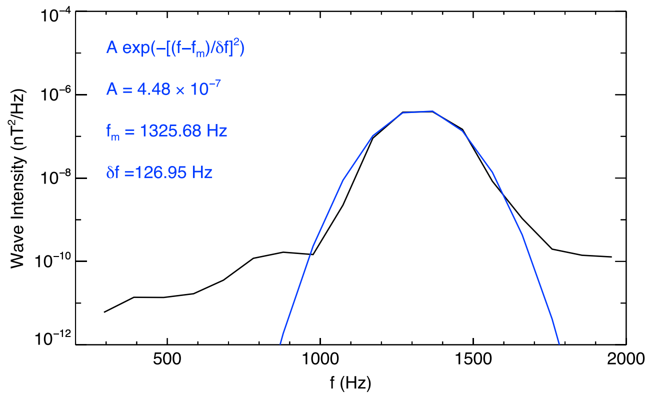


**Figure 2.** The averaged wave power distribution as a function of frequency (black) and the corresponding Gaussian fitting function (blue).

Here $A_0(t)$ and $P(t)$ represent the stochastic processes of $\alpha_0$ and $p$, respectively. The coefficients $b_{\alpha_0}$ and $b_p$ are defined by

$$b_{\alpha_0}(t,\alpha_0,p) = \frac{1}{Gp}\frac{\partial}{\partial \alpha_0}\left(\frac{GD_{\alpha_0\alpha_0}}{p}\right) + \frac{1}{G}\frac{\partial}{\partial p}\left(\frac{GD_{\alpha_0 p}}{p}\right), \quad (7)$$

$$b_p(t,\alpha_0,p) = \frac{1}{Gp}\frac{\partial}{\partial \alpha_0}\left(GD_{\alpha_0 p}\right) + \frac{1}{G}\frac{\partial}{\partial p}\left(GD_{pp}\right). \quad (8)$$

Components of matrix $\boldsymbol{\sigma}$ are related to diffusion coefficients by

$$\boldsymbol{\sigma}\boldsymbol{\sigma}^{\mathrm{T}} = \begin{pmatrix} 2D_{\alpha_0\alpha_0}/p^2 & 2D_{\alpha_0 p}/p \\ 2D_{\alpha_0 p}/p & 2D_{pp}. \end{pmatrix}, \quad (9)$$

with $\boldsymbol{\sigma}^{\mathrm{T}}$ the transpose of $\boldsymbol{\sigma}$. Note that $\boldsymbol{\sigma}$ is not uniquely defined by this equation. However, different choices of $\boldsymbol{\sigma}$ lead to equivalent stochastic processes [*Freidlin*, 1985]. By choosing $\sigma_{12} = 0$ for simplicity, we have

$$\sigma_{11} = \sqrt{2D_{\alpha_0\alpha_0}}/p, \quad (10)$$

$$\sigma_{21} = \sqrt{2}D_{\alpha_0 p}/\sqrt{D_{\alpha_0\alpha_0}}, \quad (11)$$

$$\sigma_{22} = \sqrt{2D_{pp} - \sigma_{21}^2}. \quad (12)$$

For details of the derivation of above SDEs and the time forward SDE method, we refer readers to *Tao et al.* [2008, and references therein].

To obtain electron distributions from quasilinear theory that can be compared with those from test particle simulations, we use 2000 electrons with the same initial $\alpha_0$ and momentum $p$ as those in test particle simulations. We then solve equations (5) and (6) for one unperturbed bounce period to obtain the quasilinear prediction of electron distributions. It can be noted that the SDE approach is quite similar to the direct test particle simulation except that the stochastic differential equations are solved instead of the Lorentz equations.

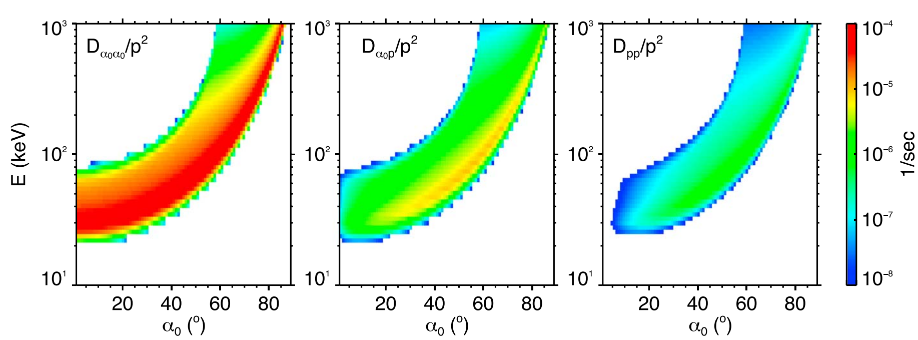


**Figure 3.** The inverse time scales ($s^{-1}$) from quasilinear diffusion coefficients as a function of equatorial pitch angle $\alpha_0$ and energy $E$.

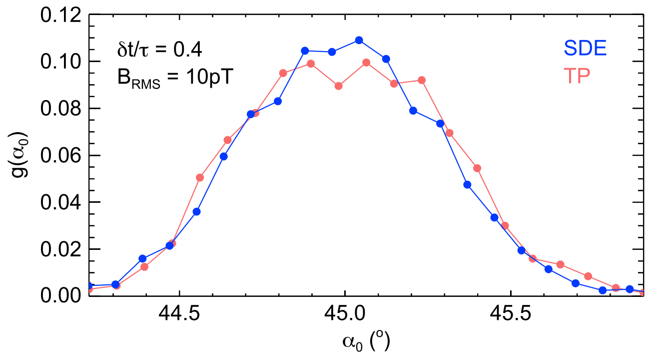


**Figure 4.** The comparison between electron distributions in $\alpha_0$ from test particle simulations (red) and from the SDE method (blue) for $\delta t/\tau = 0.4$ and $B_{\mathrm{RMS}} = 10$ pT.

## 4. Comparison With Quasilinear Theory

In this section, we apply the method outlined above and demonstrate how chorus waves consisting of coherent elements with subpacket structures affect the dynamics of energetic electrons. The effects of wave amplitude have been investigated extensively in previous work by using a single coherent wave, showing phase trapping and phase bunching if the amplitude is large enough [*Inan et al.*, 1978; *Bell*, 1984; *Omura et al.*, 2007; *Albert*, 2000; *Bortnik et al.*, 2008; *Furuya et al.*, 2008]. For broadband waves, *Tao et al.* [2012b] demonstrate that quasilinear theory overestimates diffusion coefficients if the amplitude of the wave field is too large. Here we only focus on how the discreteness of chorus elements affects the applicability of quasilinear theory by performing simulations for three different cases. For simplicity, we characterize the discreteness of chorus by $\delta t/\tau$, where $\tau \approx 0.22$ s is the duration of one element, as illustrated in Figure 1. Hence, if $\delta t/\tau > 1$, there is no overlap between any elements of chorus when generated.

### 4.1. Case 1: Small Wave Amplitude and Small $\delta t/\tau$

In Case 1, we choose $\delta t/\tau = 0.4$ and rescale the amplitude of each element of chorus so that the root-mean-squared amplitude used in the traditional quasilinear approach is $B_w = 10$ pT. To calculate the quasilinear diffusion coefficients, we model chorus as broadband whistler waves, ignoring any fine structures such as its discreteness and frequency chirping, as done by previous work [e.g., *Horne et al.*, 2005a]. Since the wave amplitude is latitude independent, we use the wave field recorded at an arbitrarily chosen latitude to obtain its time-averaged power distribution as a function of frequency shown in Figure 2. The obtained Gaussian fitting function of the wave power distribution is then used to calculate quasilinear diffusion coefficients. These diffusion coefficients, shown in Figure 3, are used in SDEs (5) and (6) to obtain stochastic trajectories of $\alpha_0$ and $p$. We compare normalized distributions of electrons in $\alpha_0$, denoted by $g(\alpha_0)$, obtained from the SDE method and the test particle simulation in Figure 4. The two distributions agree quite well, except for some statistical fluctuations due to the use of a finite number of electrons. The comparison indicates that when both $B_w$ and $\delta t/\tau$ are small, quasilinear theory can provide a good description of effects of chorus on electrons. This is reasonable because nonlinear effects are negligible when $B_w$ is small, and chorus waves can be approximated by broadband whistler waves when $\delta t$ is small for a given $\tau$. This case serves as our control case since it most closely satisfies the basic assumptions of quasilinear theory. In the next two simulation runs, we will demonstrate the effects of discreteness by using a larger value of $\delta t/\tau$.

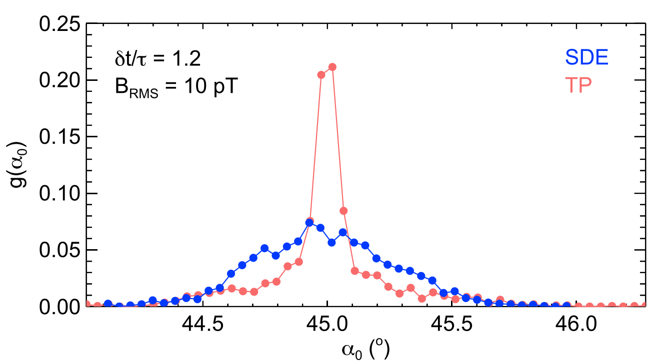


**Figure 5.** The comparison between electron distributions in $\alpha_0$ from test particle simulations (red) and from the SDE method (blue) for $\delta t/\tau = 1.2$ and $B_{\mathrm{RMS}} = 10$ pT.

### 4.2. Case 2: Small Wave Amplitude and Large $\delta t/\tau$

We now set $\delta t/\tau = 1.2$, indicating no overlap between chorus elements when generated. We rescale the amplitude of each element so that the root-mean-squared amplitude $B_w$ is still 10 pT. Because we use the same element when modeling chorus, the resulting average wave power distribution and quasilinear diffusion coefficients are the same as those in Case 1, shown in Figures 2 and 3, respectively. The electron distributions from test particle simulations

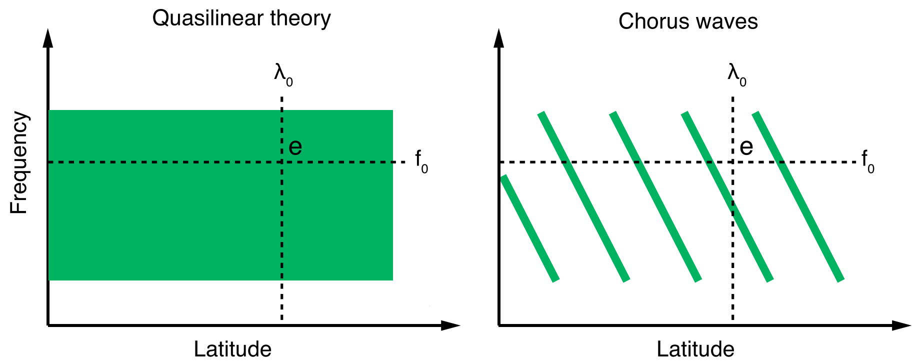


**Figure 6.** A schematic plot showing the difference in scattering of an electron resonating with a wave at frequency $f_0$ at latitude $\lambda_0$ between a broadband and continuous wave field assumed by (left) quasilinear theory and (right) a realistic chorus wave field with discrete elements.

and the SDE method are compared in Figure 5, which indicates that quasilinear theory does not describe well the effects of chorus on electrons in this case. The most prominent feature in Figure 5 is that, compared with the distribution from the SDE method, there is a bump in the distribution from the test particle simulation at $\alpha_0 = 45°$, which is the initial value of $\alpha_0$ of electrons. The difference indicates that, compared with quasilinear theory results, there are more electrons in the test particle simulation that do not get enough change in equatorial pitch angle $\alpha_0$ from scattering by chorus when $\delta t/\tau = 1.2$.

The reason for the formation of this bump is illustrated in Figure 6, which shows the distribution of waves as a function of frequency and latitude at some given time. In traditional quasilinear approach (Figure 6, left), the internal structures of chorus waves are ignored. The wave field used in the quasilinear calculation is a broadband whistler wave field with the same frequency power distribution as that of chorus. The actual chorus wave field (Figure 6, right), however, is discrete and thus different from the continuous field assumed in previous quasilinear modeling. We now consider an electron which resonates with waves at frequency $f_0$ at some latitude $\lambda_0$. In quasilinear modeling, the electron can be resonantly scattered as long as $f_0$ is within the wave frequency range. However, the electrons might miss this resonance in the realistic chorus field when the elements are widely separated. As a result, a bump in distribution around its initial phase space coordinate is formed.

### 4.3. Case 3: Large Wave Amplitude and Large $\delta t/\tau$

In Case 3, we use $\delta t/\tau = 1.2$ and rescale the amplitude of each element so that the root-mean-squared wave amplitude is 80 pT. This change of wave amplitude increases the value of diffusion coefficients D by a factor of 64, since D $\propto B_w^2$. The structure of D is still given by Figure 3.

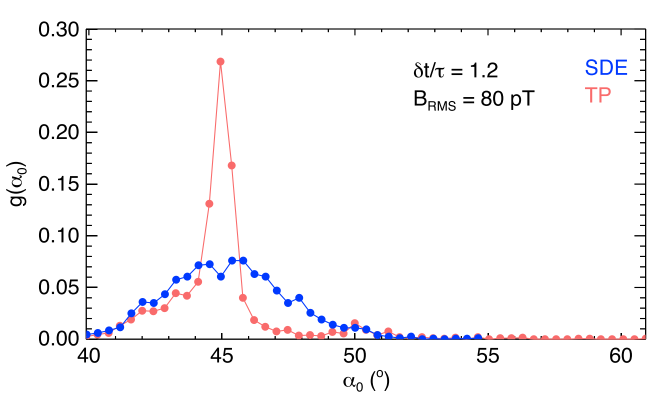


**Figure 7.** The comparison between electron distributions in $\alpha_0$ from test particle simulations (red) and from the SDE method (blue) for $\delta t/\tau = 1.2$ and $B_{RMS} = 80$ pT.

The comparison of distributions from the test particle simulation and the SDE method are given in Figure 7. In the test particle simulation results, one can see that there is still a bump in the electron distribution around $\alpha_0 = 45°$, which is due to the discreteness of chorus as explained in the previous section. Meanwhile there is a long tail of $g(\alpha_0)$ in large pitch angles ($\alpha_0 > 55°$), which is not present in the distribution from the SDE method.

We now demonstrate that these large changes of $\alpha_0$ are due to phase trapping of electrons [e.g., *Albert*, 2000; *Bortnik et al.*, 2008]. In Figure 8, we show the change of $\alpha_0$ of a randomly

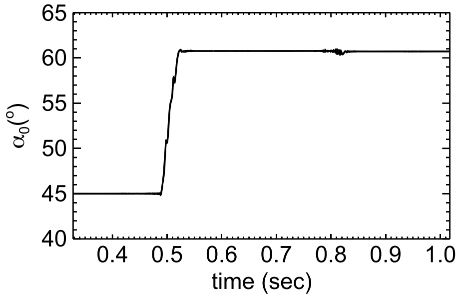


**Figure 8.** The variation of equatorial pitch angle $\alpha_0$ as a function of time of a randomly chosen particle with large variation of $\alpha_0$ from case 3.

chosen particle whose final $\alpha_0 \geq 60°$. One can clearly see that the large variation of $\alpha_0$ occurs around $t = 0.5$ s. We plot in Figure 9, the wave number ($k$), the wave frequency ($\omega$), and the wave amplitude $B_w$ seen by the particle, and $\eta \equiv \omega - kv_{\|} - |\Omega_e|/\gamma$ as a resonance indicator from $t = 0.49$ s to 0.52 s. Here $\Omega_e$ is the local cyclotron frequency of electrons and $\gamma$ is the relativistic factor. First, we demonstrate that the wave amplitude is large enough to cause phase trapping of particles. For interactions between an electron and a coherent whistler wave, the phase angle $\zeta$ between the perpendicular velocity and the wave magnetic field satisfies the second-order differential equation [*Omura et al.*, 2008],

$$\frac{d^2\zeta}{dt^2} = \frac{\omega_t^2\delta^2}{\gamma}(\sin\zeta + S)\,. \tag{13}$$

Here the inhomogeneity ratio $S$ is defined by *Omura et al.* [2008] for a constant amplitude wave with varying frequency as

$$S = -\frac{1}{\omega_t^2\delta^2}\left\{\gamma(1-\frac{v_R}{v_g})^2\frac{\partial\omega}{\partial t} + \left[\frac{\gamma k v_g^2}{2|\Omega_e|} - \left(1+\frac{\delta^2}{2}\frac{|\Omega_e|-\gamma\omega}{|\Omega_e|-\omega}\right)v_R\right]\frac{\partial|\Omega_e|}{\partial z}\right\}. \tag{14}$$

Phase trapping is possible if $|S| < 1$. In equations (13) and (14), $v_R$ is the resonant velocity of the particle, $v_g$ is the wave group velocity, $z$ is the distance along a field line from the magnetic equator, and $\omega_t = \sqrt{kv_g|\Omega_w|}$. Here $\Omega_w \equiv qB_w/mc$ is the gyrofrequency due to the wave magnetic field, and $v_g$ is particle velocity component perpendicular to the background magnetic field. Variables $q$, $m$, and $c$ have their usual means of charge, mass, and speed of light in vacuum, respectively. Variable $\delta^2$ is defined by *Omura et al.* [2008] as

$$\delta^2 = \frac{\omega_{pe}^2}{\omega_{pe}^2 + \omega(|\Omega_e| - \omega)}, \tag{15}$$

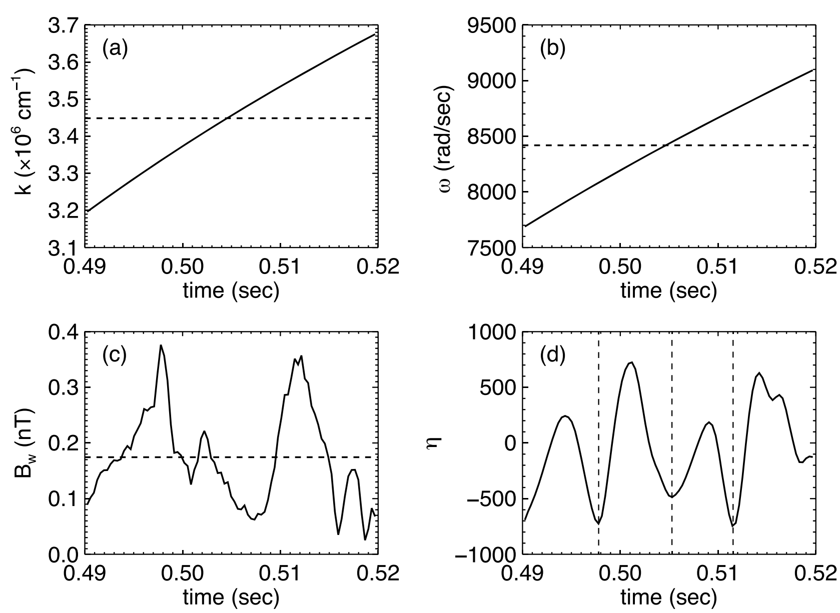


**Figure 9.** The variation of (a) wave number $k$, (b) wave frequency $\omega$, (c) wave amplitude $B_w$, and (d) $\eta \equiv \omega - kv_{\|} - |\Omega_e|/\gamma$ from $t = 0.49$ s to 0.52 s for the particle shown in Figure 8. Horizontal dashed lines in Figures 9a–9c denote the average values of the corresponding variables, and the vertical dashed lines in Figure 9d are drawn to aid the visualization of four oscillations.

where $\omega_{\mathrm{pe}}$ is the electron plasma frequency. Note that the presence of amplitude modulation complicates the calculation of $S$, so we can only make a rough estimate of $S$ by using average values, which are denoted by $\langle\cdots\rangle$, of the corresponding variables in equation (14) between $t = 0.49$ s and 0.52 s. Substituting $\langle k\rangle = 3.45 \times 10^{-6}$ cm$^{-1}$, $\langle\omega\rangle = 8418.5$ rad/s, $\langle B_w\rangle = 0.17$ nT, and $\partial|\Omega_e|/\partial z = 1.8 \times 10^{-5}$ rad $\cdot$ s$^{-1}$ $\cdot$ cm$^{-1}$ into equation (14), we have $|S| = 0.76$, which indicates that phase trapping is possible. Second, from Figure 9d, one can see the oscillation of $\eta$. We now compare the period of the oscillation of $\eta$ in Figure 9d with theoretical period of phase trapping, There are about four oscillations from $t = 0.49$ s to 0.52 s, so the oscillation period is roughly 0.0075 s. The theoretical phase-trapping frequency is about $\omega_t = \sqrt{kv_{\mathrm{g}}|\Omega_w|}$. The average perpendicular velocity of the particle from $t = 0.49$ s to 0.52 s is $\langle v_{\mathrm{g}}\rangle \approx 0.46\,c$. We can calculate that $\omega_t$ is about 1101 rad/s, using $\langle k\rangle$ and $\langle B_w\rangle$. Hence the theoretical period of phase trapping is about $T_t = 0.0057$ s, roughly consistent with the period shown in Figure 9d. Therefore, both calculations of $S$ and the oscillation period indicate that the large variations of $\alpha_0$ are caused by phase trapping of electrons by chorus waves.

In conclusion, when both $B_w$ and $\delta t/\tau$ are large, quasilinear theory does not give a good description of resonant scattering of electrons because of the nonlinear effects and the discreteness of chorus.

## 5. Discussions and Summary

In this work, we presented the use of the time forward SDE method to obtain a distribution of electrons that can be easily compared with that from test particle simulations. This method can be utilized to investigate the applicability of quasilinear theory to various wave particle interaction processes in general. Using the method, we investigated for the first time, as far as we are aware, the effect of discreteness of chorus on the dynamics of energetic electrons. We show that quasilinear theory is applicable to describe the evolution of the electron distribution when both the wave amplitude and the separation between chorus elements, quantified by $\delta t/\tau$ in this work, are small. Physically this is because the chorus field is well approximated by broadband whistler waves in this case, and nonlinear effects are ignorable. On the other hand, when $\delta t/\tau$ is large, electrons can frequently miss resonances with chorus because of its discreteness, forming a bump around their initial phase space coordinates when compared with predictions from quasilinear theory. We also demonstrated that when using a wave field with both large $\delta t/\tau$ and large amplitude, interactions with chorus created a long tail in electron pitch angle distribution due to phase trapping besides the bump around the initial pitch angle. Our results demonstrate that, while simple constant amplitude wave models are helpful to illustrate the physical mechanism involved in the electron-chorus interaction process, it is important to include realistic features of chorus waves in quantifying their effects on energetic electrons.

We should point out here a few limitations of this work. First, we performed the simulation for only one unperturbed bounce period since we are mainly interested in understanding the physical processes involved in the interactions between electrons and chorus. Whether or not long-term interactions can smooth the distribution function and reduce the effects of discreteness is yet to be determined. Second, it is important to establish the criterion to determine whether a given value of the wave amplitude or $\delta t$ is small enough for quasilinear theory to be applicable. Third, the current conclusions should be combined with the observed distribution of $\delta t$ of chorus, which is not available yet as far as we know, to determine the overall effects of chorus waves on energetic electron dynamics in the inner magnetosphere. However, these are out of scope of the current study and will be left as a future work.

**Acknowledgments**

This research was supported at UCLA by NSF grant 0903802, NASA grant NNX11AR64G, and DE-SC0010578, which was awarded through the NSF/DOE Plasma Partnership program. Xin Tao was also supported by USTC grant KY2080000018, NSFC grant 41121003, and CAS Key Research Program KZZD-EW-01-4. Jay Albert was supported by the NASA LWS TR&T program. The model data will be preserved on a long-term storage system and will be made available upon request to the corresponding author.

Michael Balikhin thanks the reviewers for their assistance in evaluating this paper.

## References

Albert, J. M. (2000), Gyroresonant interactions of radiation belt particles with a monochromatic electromagnetic wave, *J. Geophys. Res.*, *105*(A9), 21,191–21,209.

Albert, J. M., N. P. Meredith, and R. B. Horne (2009), Three-dimensional diffusion simulation of outer radiation belt electrons during the 9 October 1990 magnetic storm, *J. Geophys. Res.*, *114*, A09214, doi:10.1029/2009JA014336.

Angelopoulos, V. (2008), The THEMIS mission, *Space Sci. Rev.*, *141*, 5–34, doi:10.1007/s11214-008-9336-1.

Bell, T. F. (1984), The nonlinear gyroresonance interaction between energetic electrons and coherent VLF waves propagating at an arbitrary angle with respect to the Earth's magnetic field, *J. Geophys. Res.*, *89*(A2), 905–918.

Bellan, P. M. (2013), Pitch angle scattering of an energetic magnetized particle by a circularly polarized electromagnetic wave, *Phys. Plasmas*, *20*, 042117, doi:10.1063/1.4801055.

Birdsall, C. K., and A. B. Langdon (2004), *Plasma Physics via Computer Simulation, Series in Plasma Physics*, 1st ed., Taylor and Francis, New York.

Bortnik, J., R. M. Thorne, and U. S. Inan (2008), Nonlinear interaction of energetic electrons with large amplitude chorus, *Geophys. Res. Lett.*, *35*, L21102, doi:10.1029/2008GL035500.

Burtis, W. J., and R. A. Helliwell (1976), Magnetospheric chorus: Occurrence patterns and normalized frequency, *Planet. Space Sci.*, *24*(11), 1007–1010, doi:10.1016/0032-0633(76)90119-7.

Denton, R. E., J. Goldstein, and J. D. Menietti (2002), Field line dependence of magnetospheric electron density, *Geophys. Res. Lett.*, *29*(24), 2205, doi:10.1029/2002GL015963.

Freidlin, M. (1985), *Functional Integration and Partial Differential Equations*, Princeton Univ. Press, Princeton, N. J.

Furuya, N., Y. Omura, and D. Summers (2008), Relativistic turning acceleration of radiation belt electrons by whistler mode chorus, *J. Geophys. Res.*, *113*, A04224, doi:10.1029/2007JA012478.

Gonzalez, W. D., J. A. Joselyn, Y. Kamide, H. W. Kroehl, G. Rostoker, B. T. Tsurutani, and V. M. Vasyliunas (1994), What is a geomagnetic storm?, *J. Geophys. Res.*, *99*(A4), 5771–5792, doi:10.1029/93JA02867.

Hajra, R., B. T. Tsurutani, E. Echer, and W. D. Gonzalez (2014), Relativistic electron acceleration during high-intensity, long-duration, continuous AE activity (HILDCAA) events: Solar cycle phase dependences, *Geophys. Res. Lett.*, *41*, 1876–1881, doi:10.1002/2014GL059383.

Horne, R. B., R. M. Thorne, S. A. Glauert, J. M. Albert, N. P. Meredith, and R. R. Anderson (2005a), Timescale for radiation belt electron acceleration by whistler mode chorus waves, *J. Geophys. Res.*, *110*, A03225, doi:10.1029/2004JA010811.

Horne, R. B., et al. (2005b), Wave acceleration of electrons in the Van Allen radiation belts, *Nature*, *437*, 227–230, doi:10.1038/nature03939.

Hospodarsky, G. B., T. F. Averkamp, W. S. Kurth, D. A. Gurnett, J. D. Menietti, O. Santoík, and M. K. Dougherty (2008), Observations of chorus at Saturn using the Cassini Radio and Plasma Wave Science instrument, *J. Geophys. Res.*, *113*, A12206, doi:10.1029/2008JA013237.

Inan, U. S., T. F. Bell, and R. A. Helliwell (1978), Nonlinear pitch angle scattering of energetic electrons by coherent VLF waves in the magnetosphere, *J. Geophys. Res.*, *83*(A7), 3235–3253.

Kennel, C. F., and F. Engelmann (1966), Velocity space diffusion from weak plasma turbulence in a magnetic field, *Phys. Fluids*, *9*(12), 2377–2388.

Kersten, K., et al. (2011), Observation of relativistic electron microbursts in conjunction with intense radiation belt whistler-mode waves, *Geophys. Res. Lett.*, *38*, L08107, doi:10.1029/2011GL046810.

Lauben, D. S., U. S. Inan, T. F. Bell, D. L. Kirchner, G. B. Hospodarsky, and J. S. Pickett (1998), VLF chorus emissions observed by Polar during the January 10, 1997, magnetic cloud, *Geophys. Res. Lett.*, *25*(15), 2995–2998, doi:10.1029/98GL01425.

LeDocq, M. J., D. A. Gurnett, and G. B. Hospodarsky (1998), Chorus source locations from VLF Poynting flux measurements with the Polar spacecraft, *Geophys. Res. Lett.*, *25*(21), 4063–4066, doi:10.1029/1998GL900071.

Li, W., Y. Y. Shprits, and R. M. Thorne (2007), Dynamic evolution of energetic outer zone electrons due to wave-particle interactions during storms, *J. Geophys. Res.*, *112*, A10220, doi:10.1029/2007JA012368.

Lorentzen, K. R., J. B. Blake, U. S. Inan, and J. Bortnik (2001), Observations of relativistic electron microbursts in association with VLF chorus, *J. Geophys. Res.*, *106*(A4), 6017–6027.

Nishimura, Y., et al. (2010), Identifying the driver of pulsating aurora, *Science*, *330*(6000), 81–84, doi:10.1126/science.1193130.

O'Brien, T. P., M. D. Looper, and J. B. Blake (2004), Quantification of relativistic electron microburst losses during the GEM storms, *Geophys. Res. Lett.*, *31*, L04802, doi:10.1029/2003GL018621.

Omura, Y., N. Furuya, and D. Summers (2007), Relativistic turning acceleration of resonant electrons by coherent whistler mode waves in a dipole magnetic field, *J. Geophys. Res.*, *112*, A06236, doi:10.1029/2006JA012243.

Omura, Y., Y. Katoh, and D. Summers (2008), Theory and simulation of the generation of whistler-mode chorus, *J. Geophys. Res.*, *113*, A04223, doi:10.1029/2007JA012622.

Reeves, G. D., et al. (2013), Electron acceleration in the heart of the Van Allen radiation belts, *Science*, *341*(6149), 991–994, doi:10.1126/science.1237743.

Roederer, J. G. (1970), *Dynamics of Geomagnetically Trapped Radiation, Physics and Chemistry in Space*, vol. 2, Springer, Berlin.

Saito, S., Y. Miyoshi, and K. Seki (2012), Relativistic electron microbursts associated with whistler chorus rising tone elements: GEMSIS-RBW simulations, *J. Geophys. Res.*, *117*, A10206, doi:10.1029/2012JA018020.

Santolík, O., D. A. Gurnett, J. S. Pickett, M. Parrot, and N. Cornilleau-Wehrlin (2003), Spatio-temporal structure of storm-time chorus, *J. Geophys. Res.*, *108*(A7), 1278, doi:10.1029/2002JA009791.

Santolík, O., D. A. Gurnett, J. S. Pickett, M. Parrot, and N. Cornilleau-Wehrlin (2004), A microscopic and nanoscopic view of storm-time chorus on 31 March 2001, *Geophys. Res. Lett.*, *31*, L02801, doi:10.1029/2003GL018757.

Su, Z., H. Zheng, and S. Wang (2009), Evolution of electron pitch angle distribution due to interactions with whistler mode chorus following substorm injections, *J. Geophys. Res.*, *114*, A08202, doi:10.1029/2009JA014269.

Subbotin, D., Y. Shprits, and B. Ni (2010), Three-dimensional VERB radiation belt simulations including mixed diffusion, *J. Geophys. Res.*, *115*, A03205, doi:10.1029/2009JA015070.

Tao, X., A. A. Chan, J. M. Albert, and J. A. Miller (2008), Stochastic modeling of multidimensional diffusion in the radiation belts, *J. Geophys. Res.*, *113*, A07212, doi:10.1029/2007JA012985.

Tao, X., R. M. Thorne, W. Li, B. Ni, N. P. Meredith, and R. B. Horne (2011a), Evolution of electron pitch-angle distributions following injection from the plasma sheet, *J. Geophys. Res.*, *116*, A04229, doi:10.1029/2010JA016245.

Tao, X., J. Bortnik, J. M. Albert, K. Liu, and R. M. Thorne (2011b), Comparison of quasilinear diffusion coefficients for parallel propagating whistler mode waves with test particle simulations, *Geophys. Res. Lett.*, *38*, L06105, doi:10.1029/2011GL046787.

Tao, X., J. Bortnik, R. M. Thorne, J. Albert, and W. Li (2012a), Effects of amplitude modulation on nonlinear interactions between electrons and chorus waves, *Geophys. Res. Lett.*, *39*, L06102, doi:10.1029/2012GL051202.

Tao, X., W. Li, J. Bortnik, R. M. Thorne, and V. Angelopoulos (2012b), Comparison between theory and observation of the frequency sweep rates of equatorial rising tone chorus, *Geophys. Res. Lett.*, *39*, L08106, doi:10.1029/2012GL051413.

Thorne, R. M., T. P. O'Brien, Y. Y. Shprits, D. Summers, and R. B. Horne (2005), Timescale for MeV electron microburst loss during geomagnetic storms, *J. Geophys. Res.*, *110*, A09202, doi:10.1029/2004JA010882.

Thorne, R. M., B. Ni, X. Tao, R. B. Horne, and N. P. Meredith (2010), Scattering by chorus waves as the dominant cause of diffuse auroral precipitation, *Nature*, *467*, 943–946, doi:10.1038/nature09467.

Thorne, R. M., et al. (2013), Rapid local acceleration of relativistic radiation-belt electrons by magnetospheric chorus, *Nature*, *504*, 411–414, doi:10.1038/nature12889.

Tsurutani, B. T., and E. J. Smith (1974), Postmidnight chorus: A substorm phenomenon, *J. Geophys. Res.*, *79*(1), 118–127.

Tsurutani, B. T., and E. J. Smith (1977), Two types of magnetospheric ELF chorus and their substorm dependences, *J. Geophys. Res.*, *82*(32), 5112–5128, doi:10.1029/JA082i032p05112.

Tsurutani, B. T., O. P. Verkhoglyadova, G. S. Lakhina, and S. Yagitani (2009), Properties of dayside outer zone chorus during HILDCAA events: Loss of energetic electrons, *J. Geophys. Res.*, *114*, A03207, doi:10.1029/2008JA013353.

Tsurutani, B. T., B. J. Falkowski, O. P. Verkhoglyadova, J. S. Pickett, O. Santolík, and G. S. Lakhina (2011), Quasi-coherent chorus properties: 1.Implications for wave-particle interactions, *J. Geophys. Res.*, *116*, A09210, doi:10.1029/2010JA016237.
Tsurutani, B. T., G. S. Lakhina, and O. P. Verkhoglyadova (2013), Energetic electron ($>$ 10keV) microburst precipitation, $\sim 5-15$s X-ray pulsations, chorus, and wave-particle interactions: A review, *J. Geophys. Res. Space Physics*, *118*, 2296–2312, doi:10.1002/jgra.50264.
Walker, A. (1993), *Plasma Waves in the Magnetosphere, Physics and Chemistry in Space*, [Germany], Springer, Berlin.
Xiao, F., Z. Su, H. Zheng, and S. Wang (2010), Three-dimensional simulations of outer radiation belt electron dynamics including cross-diffusion terms, *J. Geophys. Res.*, *115*, A05216, doi:10.1029/2009JA014541.